Enhancing Residential Sustainability: Multi-objective optimization of hydrogen-based multi-energy system

Mathieu Patin, Sylvie Bégot, Frédéric Gustin, Valérie Lepiller

Enhancing Residential Sustainability: Multi-objective optimization of hydrogen-based multi-energy system

Mathieu PATIN[1a], Sylvie BEGOT[1], Frédéric GUSTIN[1], Valérie LEPILLER[1]

[1]Université de Franche-Comté, FEMTO-ST, FCLAB, UTBM, CNRS, Belfort, France

[a]mathieu.patin@femto-st.fr ; 13 rue Ernest Thierry-Mieg, 90010 Cedex Belfort, France

Abstract

To enhance residential sustainability by providing decarbonized and locally produced energy to a residential district, the relevance of a grid-connected multi-energy system, including PV panels, a battery, an electrolyzer, a hydrogen tank, and a fuel cell, is studied. A model is developed that creates high-resolution, continuous yearly profiles. The model is then utilized in a metaheuristic multi-objective optimization based on total cost and life cycle greenhouse gas emissions to highlight sizing trends. In the results, the most cost-efficient solutions rely mostly on PV power with minimal battery storage capacity, whereas hydrogen systems are necessary to achieve the best emission reductions. The analysis does not identify a promising prospect for seasonal energy storage with the current tank and battery lifetime emissions. Producing more than 65% of the energy demand locally is not deemed beneficial.

Graphical abstract

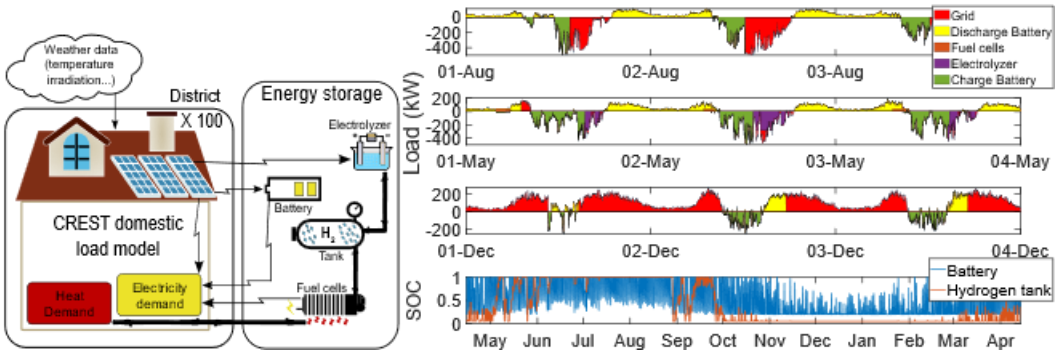

Highlights

*Modeling of annual stochastic, high-resolution, and coherent domestic load profiles.

*Modeling of a multi-energy system directly coupled with the domestic load model.

*Metaheuristic cost and emission optimization of a hydrogen-based multi-energy system.

*Seasonal energy storage does not perform well on the life cycle emission side.

*Hydrogen systems perform well on the emission side but are not currently cost-effective.

Keywords: Multi-energy, Hydrogen, Cogeneration, Domestic load modeling, Power-to-Power, Energy storage

Nomenclature

Symbols

η	Efficiency
μ	Efficiency temperature coefficient
T	Temperature (K)
G	Irradiance (W/m^2)
A	Area (m^2)
P	Power (W)
$\dot{m}$	Masse flow rate (kg/s)
HHV	Higher Heating Value (J/kg)
Q	Energy capacity (kWh)
C	Cost
G	Gain
Obj	Objectif
Em	Emission

Indices

mp	Maximum power point
ref	Reference
panel	Panel
amb	Ambient
NOCT	Normal Operating Cell Temperature
H_2	Dihydrogen
pro	Produced
cons	consume
elec	electrical

ther	thermal
bat	Battery
inv	Investment
rep	Replacement
hp	Heat pump
prov	Provided
absorb	Absorbable
hw	Hot Water

Abbreviations

BAT	Battery
EC	Electrolyzer
PV	Photovoltaics
FC	Fuel Cell
CHP	Combined Heat and Power
GA	Genetic Algorithm
PSO	Particle Swarm Optimization
CREST	Centre for Renewable Energy Systems Technology
COP	Coefficient Of Performance
EER	Energy Efficiency Ratio
PEM	Proton Exchange Membrane
SOC	State Of Charge
CAPEX	Capital expenditure
OPEX	Operating expenditure
O&M	Operation and Maintenance
kg CO_2-eq	Kilogram of CO_2 equivalent

1. Introduction

The risks associated with climate change and global warming are increasingly well-known and quantified. Under the progressive pressure from actors in the field, these climate issues are taking on an ever more important role in future policies. Initiated during climate summits (Kyoto, Copenhagen, Paris…), action plans primarily focus on reducing greenhouse gas emissions.

Around the world, buildings represent one of the most energy-intensive sectors. Responding to climate change issues must, therefore, include a reduction in this sector, through both a reduction in consumption and a decrease in the use of high-carbon energy sources such as natural gas. The natural gas supply crises in Europe have also demonstrated the need for a transition to local energy production.

To meet the demand of buildings in a decarbonized and decentralized way, the production of energy from renewable sources is a commonly used solution, especially solar photovoltaic electricity production and solar thermal hot water production. However, these energy sources are intermittent and, therefore, cannot alone cover the entire building load.

Numerous energy storage solutions are being explored for this purpose. The work presented here focuses on multi-energy systems for residential applications using both a battery (BAT) and water electrolyser (EC) to valorize the surplus electricity produced by solar photovoltaic (PV) panels by generating dihydrogen. This dihydrogen can then be used in a fuel cell (FC) during periods of low solar irradiation.

Fuel cells emit significant among of heat during operation. It is estimated that in a fuel cell stack, about 50% of the energy input is transformed into electricity, and 50% is lost as heat [1]. Valorizing this heat is, therefore, of major importance to this type of system. One solution is to use the generated heat as a source in another generation system [2, 3, 4, 5] . Some other studies focus on recovering the heat to directly improve the efficiency of the stack itself [1]. This heat can also be used to produce cold [3, 6, 7, 8].

A common use of the fuel cell's waste heat is combined heat and power (CHP). It consists of using the heat directly to meet heating needs. In residential applications, it is especially interesting because of the significant local heat needs linked to the demand for space heating and hot water production. CHP systems exist in different sizes, and micro CHP meets the demand for small applications like a single building.

Fuel cell-based micro CHP can be supplied by natural gas. Maleki et al. studied a PV/wind/FC grid-connected system for a house in Iran [9]. They modeled the system with and without heat recovery and with and without heat storage. They optimized based on economic factors and concluded that the system appears more promising with heat recovery but without heat storage. They also highlighted that the genetic algorithm (GA) performs better than particle swarm optimization (PSO). At the district size, Tooryan et al. [8], studied a PV/FC/BAT/boiler micro-grid system for the electricity, heat, and cold demand of a 300 to 500 household district. The system is optimized using PSO, and significant gas consumption reduction is achieved, especially when the fuel cell waste heat is used.

For better performance in terms of CO_2 emissions, other studies use fuel cells supplied by non-carbon-based energy sources like dihydrogen. Chang et al. studied the performances of this type of system for a house in north China [10]. The authors tested the performances with and without a battery and found a clear advantage to using a battery.

In both cases above, the micro CHP's fuel was imported but it is also possible to produce it locally. Hosseini et al. study the energy and exergy efficiency of a micro CHP system to meet the demand for an off grid single family Canadian house [11]. The systems use PV daytime excess electricity in an electrolyzer to produce H_2. Hydrogen then used in a fuel cell-based CHP.

At the district size, Arsalis et al. modeled a PV/EC/FC system meeting the total annual electricity and heating needs [12]. They used hourly data corresponding to load varying from 1 house to 100 and studied the economic performances of a system with fixed sizes. Their results indicate an interesting prospect for a hydrogen-based energy storage at the residential district level even without using the fuel cell heat.

Gabrielli et al. studied a small district of 24 buildings, including houses and commercial/office buildings [13, 14]. Using 2 criteria, cost and CO_2 emissions, the authors optimized the sizes of the components and their presence or not. Their results show that the best configuration for the CO_2 criteria consists of a PV/BAT/EC/FC system but that the hydrogen systems do not perform as well for the cost criteria, highlighting the importance of environmental analysis to fully study the benefits of this type of system.

In most studies of residential hydrogen-based multi-energy systems, the buildings' load is considered only as a decoupled input, meaning that the multi-energy systems have no influence on the buildings' thermal behavior [7, 9, 10, 11, 12, 13, 14, 15, 16, 17] [18, 19, 20, 21, 22]. Furthermore, references presented use a time step size above 1 minute, an hourly time step for [10, 11, 12, 13, 14, 17, 18, 20, 21, 22] [23, 24], half-hourly for [15, 25], 10 minutes for [7], 6 minutes for [9], and 3 minutes (hourly domestic load) [16].

Moreover, the systems' environmental impacts are often estimated but not used as optimization objectives [20, 8]. The mono-objective optimization studies often focus on economic criteria like the total systems cost or the cost of energy [7, 8, 9, 17, 18, 23, 24], which can include environmental impact but only through carbon taxes [22]. The multi-objectives optimization combine economic criteria with technical criteria (loss of power likelihood, capacity shortage, electrical production…) [19, 20] or environmental criteria (greenhouse emissions, NOx emission, land use, water consumption…) [13, 14, 16, 19]. But for greenhouse emissions, consider it only through the system operation life emissions (emission avoided by providing low-carbon energy) [13, 14, 16, 22] , which tends to favor larger configurations without taking into account the negative impacts those systems create through material extraction, assembly, transport, dismantling, etc. On the other hand, a life cycle analysis considers those impacts penalizing oversized systems.

Therefore, there is a lack of high time resolution modeling that includes the coupling between the hydrogen-energy systems and the buildings as well as a lack of multi-objective optimization using total systems life cycle assessment as a criterion. The novelty this paper aims to provide are:

- The optimization of an energy system coupled with the buildings' thermal behaviors,
- The optimizing a grid-connected PV/FC/EC/battery cogeneration system with high time resolution,
- The analysis of the change in sizing philosophy caused by optimizing on life cycle greenhouses emissions instead of operation life emissions.

For this, the following objectives needed to be accomplished:

- Model a residential district electricity, hot water, space heating and cooling demand high time resolution,

- Model a district size grid-connected PV/FC/EC/battery cogeneration system to meet these demands,
- Fully couple the energy systems with the building's thermal behaviors,
- Conduct a multi-objectives optimization of the energy systems on the total system cost and the total system life cycle greenhouse emissions,
- Investigate sizing philosophy that transpires from the optimized configurations.

2. Method

2.1. Residential load modeling

With the goal of achieving high-resolution load modeling that can be coupled with the multi-energy system, the choice was made to base the work on the model created by the Centre for Renewable Energy Systems Technology (CREST). This model is widely used in the literature and is available as an open-source VBA code. The developed model is based on statistics to stochastically produce scenarios of occupancy and consumption in the house [26]. This research group have been improving the model incrementally since the first publication in 2008. Initially, only a domestic occupancy model, it then evolved into an electricity demand model, and with the introduction of a thermal part (heating and more recently cooling), it finally became an energy domestic demand model [26, 27, 28, 29].

The model produces load curves that are both coherent and high resolution. They are coherent because all the profiles are dependent on each other, which means that, for example, when solar irradiation decreases, a simultaneous decrease in PV production and an increase in demand linked to lighting and space heating happen. High resolution is achieved because the profiles have a one-minute time step, allowing for a more precise consideration of the buildings and system's components dynamics.

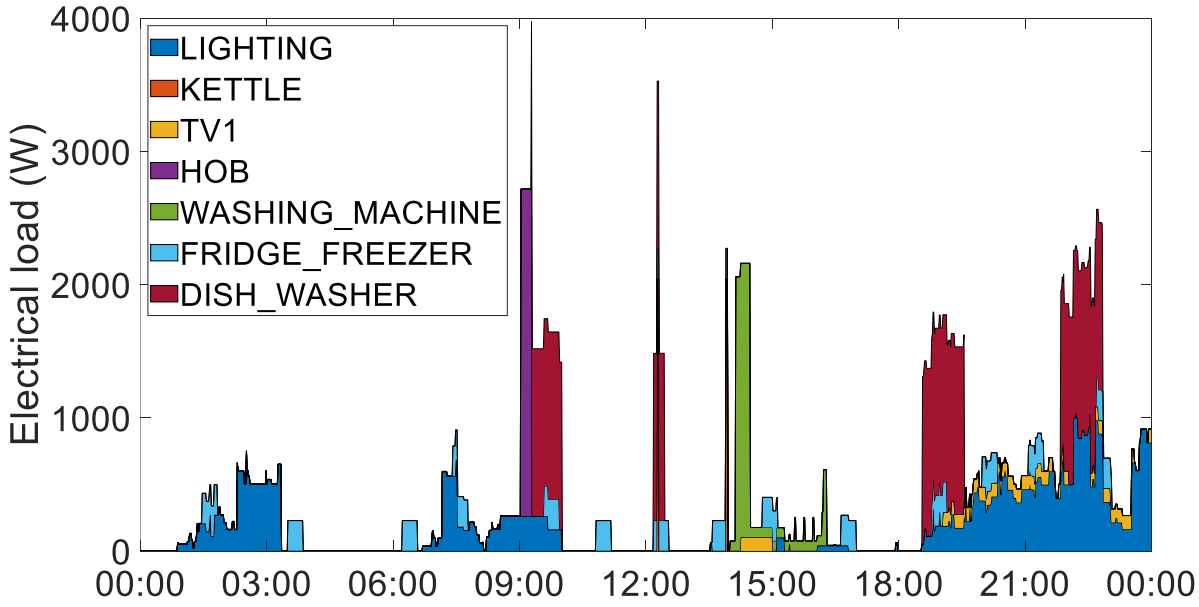

Figure 1. Electric load generated from the model with a few selected appliances

For the electrical part, the model stochastically constructs behavior patterns (occupancy, appliance usage, lighting usage, heating/cooling habits, etc.). These patterns, combined with appliance and lightbulb characteristics, produce a stochastically created electrical load profile (Fig. 1).

For the thermal part, the CREST model uses a gray box approach. Fig. 2 summarizes the thermal model [26]. The gray box model provides the temperature evolution of the house with a one-minute resolution. This evolution determines the gas or electricity consumption of the heating/cooling appliances. The gray box model approach leads to fast computation and therefore allows the coupling of the thermal model with the hydrogen cogeneration systems. Thus, the impact of the hydrogen system on the house's thermal behaviors is studied in the present work.

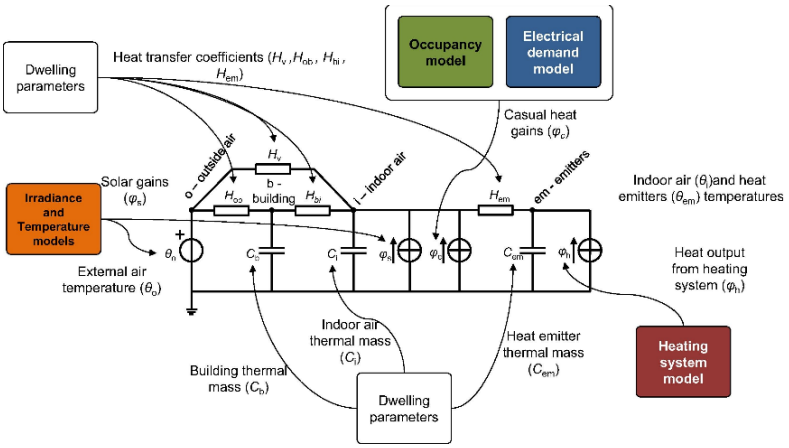

Figure 2 – Thermal part of the CREST model, from [26]

For the need of the present study, the CREST model was reimplemented from Excel VBA to the MATLAB environment. Modifications were made to allow the program to run over a specified time duration instead of only one given day, which is essential for studying the continuous behavior and energy exchange dynamics that may occur after several weeks. This also reduces the impact of the artifacts present in the first simulation's time steps due to initialization and avoids discontinuity between days.

To achieve this, the entire time loop was altered to stop after a chosen number of iterations instead of 1440 for each minute of the day. The external temperature modeling is most impacted by these changes. While the reference model calculates overnight cooling using the maximal and minimal temperature of the day D, the modified model now uses the maximal temperature of the day D and the minimal temperature for the next day D+1 to avoid discontinuity at midnight.

The heating systems modeling was also modified to replace the boilers with heat pumps, with a coefficient of performance (COP) variation according to Fig. 3 (data from [30] for an operating temperature of 55°C). Additionally, the model includes coupling with the hydrogen and battery systems. To enable this coupling, changes were made in how the model estimates the maximal power available for heating. In contrast to the reference model, where the total available power for heating was the maximum power of the building heating equipment, in this model, it now increases depending on the fuel cell production.

The building's parameters originate directly from the CREST model and thus represent medium-sized one-family detached houses situated in Great Britain. Table 1 summarizes the parameters. To simulate the whole neighborhood load, 100 different houses are modeled with the stochastic model.

Table 1 – Houses Parameters and resulting consumption

Parameter	Value	Reference
Houses area	136 m^2	[26]
Resident number	1 to 5	[26]
Climate zone	Warwick, UK	[26]
Isolation	Default CREST isolation	[26]
Average appliances consumption	3298 kWh/year	
Average lighting consumption	725 kWh/year	

Average hot water consumption	2449 kWh/year	
Average space heating consumption	89.6 kWh/year/m²	
Average space cooling consumption	19 kWh/year	
Heat pump heating capacity	23.50 kW	[30]
Heat pump nominal COP	4.3	[30]
Heat pump nominal EER	4.2	[30]

The thermal load of habitations can be fulfilled by either electrical systems like heat pumps, thermal systems like natural gas boilers or even by an urban heat network. In the current study heat pumps and the fuel cell will fulfill the thermal load. Thus, without the multi-energy system, the buildings modeled get their energy only from two sources: the electrical grid and the production of PV panels.

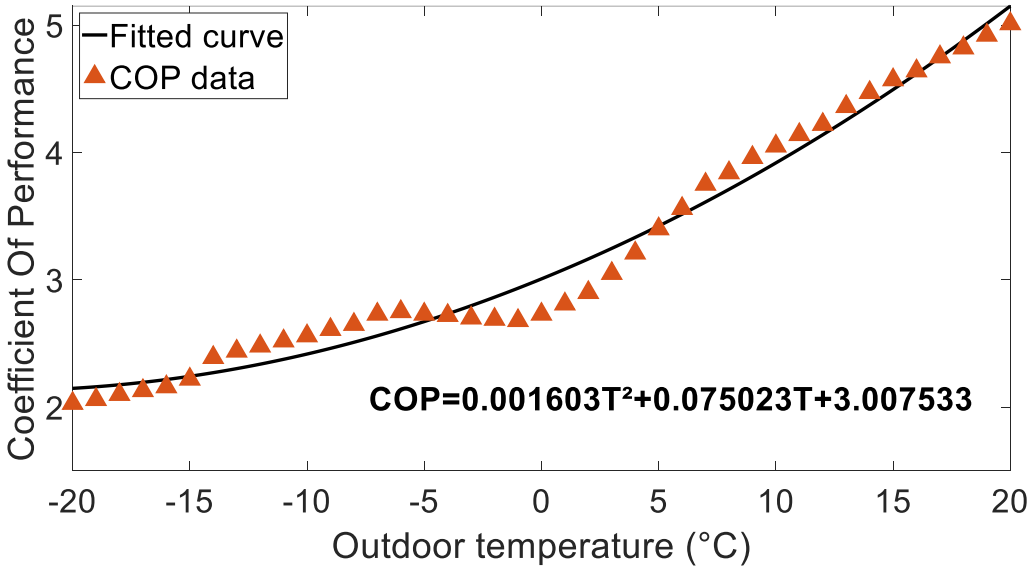

Figure 3. Heat pump COP depending on outdoor temperature, data from [30]

2.2. Multi-energy system modeling and operational strategies

2.2.1. Architecture

The system is placed at a district level and interacts with the 100 houses. It provides electricity and heat to the buildings using the overproduction created by the PV panels during the day. This overproduction is absorbed in two loops: the battery loop and the hydrogen loop. The battery loop is simply composed of the battery that is charged or discharged depending on the available electricity.

The hydrogen loop is more complex and is composed of three major subsystems and their auxiliaries. First, the electrolyzer produces dihydrogen from electricity and water, then the hydrogen tank stores this dihydrogen. Finally, the fuel cell uses it to produce heat and electricity that is transmitted to the building via a heat network and an electricity network. Fig. 4 details the link between the components and the power and heat converter used in the systems.

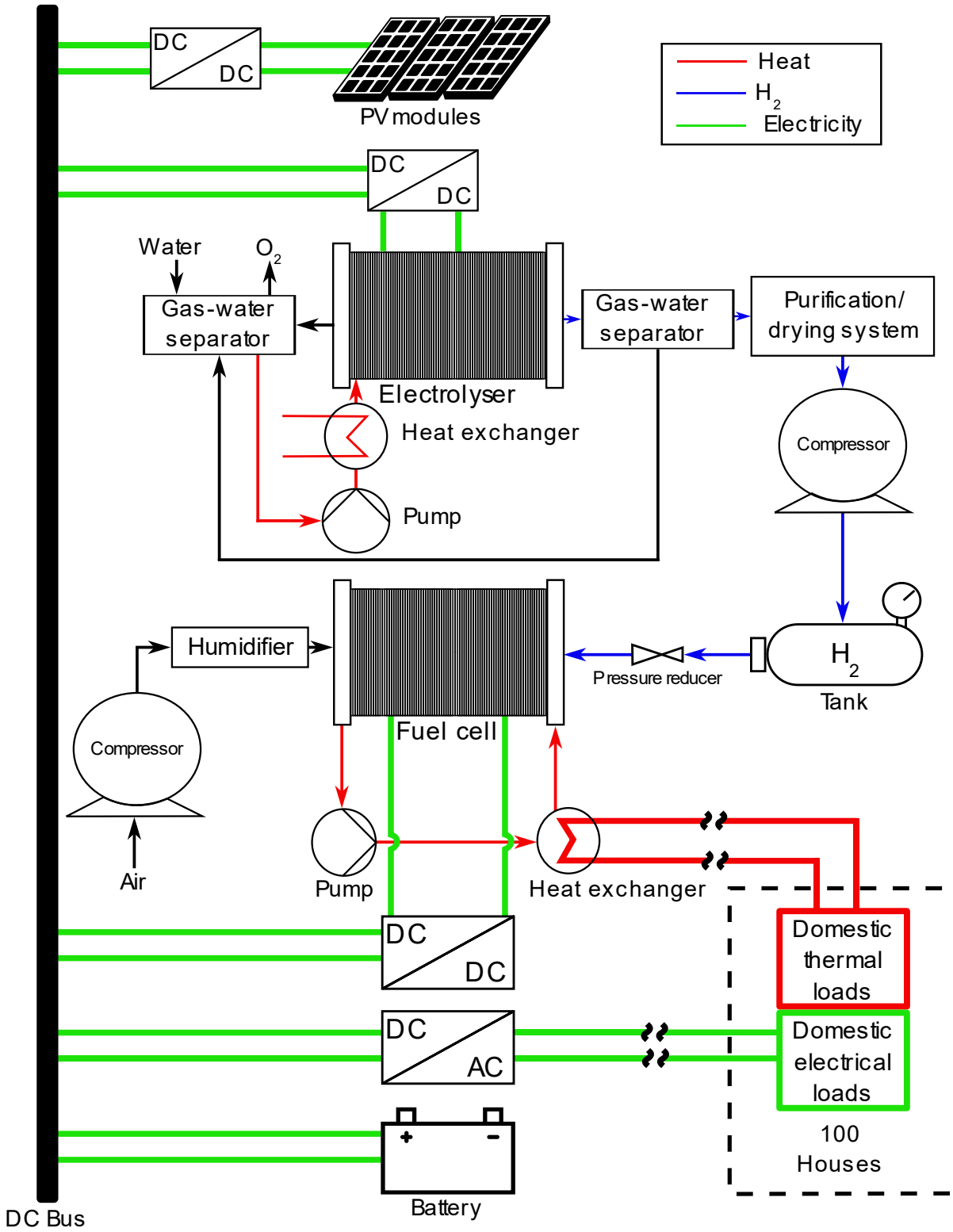

Figure 4. Detailed diagram of the multi-energy system

2.2.2. Models

To enable optimization within a realistic time frame, fast computing is essential. Therefore, opting for simplified models for all elements, with a focus on system efficiency, quantifying losses in the systems and the consumption of auxiliaries, becomes crucial.

2.2.2.1. Photovoltaic Panels

The calculation of PV panel production was modified compared to the base CREST model to incorporate the effect of the panel's temperature on efficiency. The panel efficiency is modulated according to the model used by Arsalis et al. [12]. Eq. 1 calculates the change in efficiency with temperature based on the panel's maximum power point efficiency temperature coefficient (μ_{mp}). Temperature is estimated using irradiance and panel characteristics (Eq. 2). Finally, the power produced with the modulated efficiency is given by Eq. 3.

$$\eta_{pv} = \eta_{pv,ref} \cdot \left(1 + \mu_{mp} \cdot \left(T_{panel} - T_{amb,NOCT}\right)\right) \quad (1)$$

$$\frac{T_{panel} - T_{amb}}{T_{NOCT} - T_{amb,NOCT}} = \frac{G}{G_{ref}} \cdot \left(1 - \frac{\eta_{pv,ref}}{0.9}\right) \quad (2)$$

$$P_{pv} = A_{pv,array} \cdot \mathrm{G} \cdot \eta_{pv} \quad (3)$$

2.2.2.2. Electrolyzer

The electrolyzer absorbs electricity to convert water into hydrogen. The model, based on the work of Ghenai et al. [31]. For a given power, the corresponding hydrogen mass flow rate is calculated with the higher heating value and the electrolyzer's efficiency (Eq. 4). The efficiency varies with the load factor of the electrolyzer according to the curve in Fig. 5 extracted from [32].

$$\dot{\mathrm{m}}_{H_2,prod} = \frac{\eta_{EC} \cdot P_{EC}}{HHV_{H_2}} \quad (4)$$

The electrolyzer produces hydrogen at a pressure of 50 bars. The compressed hydrogen tank stores the hydrogen at this same pressure. Therefore, additional energy losses associated with hydrogen compression or the hydrogen tank, in general, are not considered.

2.2.2.3. Fuel cells

Fuel cells utilize stored hydrogen to generate electricity and heat. The electricity and heat production of the fuel cells is modeled using an approach similar to that of Ranjbar and Kouhi [33] but with different efficiency data. The load curve employed in this study is illustrated in Fig. 6 and is adapted from [34]. In their research, a part-load curve is utilized to determine the electrical and thermal efficiency of fuel cells for a given load factor. For a specified electrical or thermal power requirement, Eq. (5) and (6) provide the hydrogen mass consumed using these efficiencies.

$$\dot{m}_{H_2,cons} = \frac{P_{elec,FC}}{HHV_{H_2} \cdot \eta_{elec,FC}} \quad (5)$$

$$\dot{m}_{H_2,cons} = \frac{P_{ther,FC}}{HHV_{H_2} \cdot \eta_{ther,FC}} \quad (6)$$

Constraints are applied to the hydrogen component's operation to simulate the dynamic limitations of real-life systems. Firstly, the electrolyzer and fuel cells operate within a specific load range; if the power provided/needed is too high, these components only absorb/provide power up to their limits. Similarly, if the power provided/needed is too low, the systems will not function, and the electrical grid or the battery will need to compensate.

Secondly, the electrolyzer and fuel cells dynamics are modeled with four phases: start-up, operating, standby, and shutdown. These phases introduce a delay between the time when the systems are activated and when they become fully operational. Although these phases constrain the reactivity of the systems, the power consumption associated with these phases is disregarded. The number of start-stop cycles negatively impacts the aging of such systems [35, 36], emphasizing the importance of minimizing these cycles. To achieve this, a standby time of one hour is implemented for the electrolyzer to delay the shutdown cycle in case excess power rises again above its minimal threshold.

To enhance system dynamics and mitigate the impact of these effects on performance, proton-exchange membrane (PEM) fuel cells and electrolyzers are chosen. This technology allows for a broader load range and shorter start/stop cycles compared to other commercial technologies (solid oxide, alkaline) [37]. Additionally, these technologies feature faster power ramping, enabling them to accommodate the highly variable residential load and PV production.

2.2.2.4. Battery

The battery serves the dual purpose of storing and providing electricity, leveraging its superior dynamics and load flexibility to balance the system. The model is based on the work of Ghenai and Bettayeb [15]. The battery's state of charge (SOC) is determined at each time step using the previous SOC and the energy charged and discharged during the time step (Eq. 7). To enhance battery lifetime, discharge is limited to a specified depth of discharge (Eq. 8). Additionally, the maximum charge and discharge power of the battery are constrained (Eq. 9 and 10).

$$SOC(t) = \mathrm{SOC}(\mathrm{t} - \Delta\mathrm{t}) + \frac{\eta_{charge} * P_{bat,charge} * \Delta t}{Q_{bat}} - \frac{\eta_{discharge} * P_{bat,discharge} * \Delta t}{Q_{bat}} \quad (7)$$

$$\begin{cases} SOC_{min} \leq SOC \leq 1 \\ SOC_{min} = (1 - DOD) \end{cases} \quad (8)$$

$$0 \leq P_{bat,charge} \leq P_{bat,max} \quad (9)$$

$$0 \leq P_{bat,discharge} \leq P_{bat,max} \quad (10)$$

In line with existing literature, the parameters for these models are established, and a concise overview is provided in Table 2. Five values are not defined in this table and correspond to the optimization variables: PV size per houses, fuel cells/electrolyzer nominal power and the storing capacity of the battery/hydrogen tank.

Some of these values can be commented. A state-of-the-art PEM electrolyzer can handle loads ranging from 0 to 120% of its nominal power and start in around 20 minutes [38]. However, aligning with the designated reference electrolyzer [32], the decision is to utilize it for loads ranging from 25 to 100%, incorporating a start-up time of 30 minutes. The chosen start-up time for the PEMFC is intentionally greater than reported in [37] to account for the thermal inertia.

Table 2 – Hydrogen CHP system parameters

Parameter	Value	Reference
PV area	**To optimize**	
PV nominal efficiency	16.9%	[11]
PV slop	40°	
PV direction	South	
PV efficiency temperature coefficient	-0.38%/°C	[11]
Electrolyzer nominal power	**To optimize**	
Electrolyzer efficiency	65–75% (cf. Fig. 5)	[32]
Electrolyzer load range	25–100%	
Electrolyzer start-up delay	30 minutes	
Electrolyzer shutdown delay	11 minutes	
Fuel cells nominal power	**To optimize**	
Fuel cells electric efficiency	20–30% (cf. Fig. 6)	[34]
Fuel cells thermal efficiency	15–45%	[34]
Fuel cells load range (electric)	13–100%	[34]
Fuel cells start-up delay	5 minutes	
Fuel cells shutdown delay	0 minutes	
Hydrogen tank capacity	**To optimize**	
Battery capacity	**To optimize**	
Battery Depth of Discharge	80%	[39]
Battery max charging rate	1C	
Battery max discharging rate	1C	
Battery charge efficiency	92%	[39]
Battery discharge efficiency	92%	[39]
DC/DC converter efficiency	95%	[40]
DC/AC converter efficiency	95%	[40]
Heat exchanger efficiency	85%	[41]
Heat network efficiency	80%	[42]

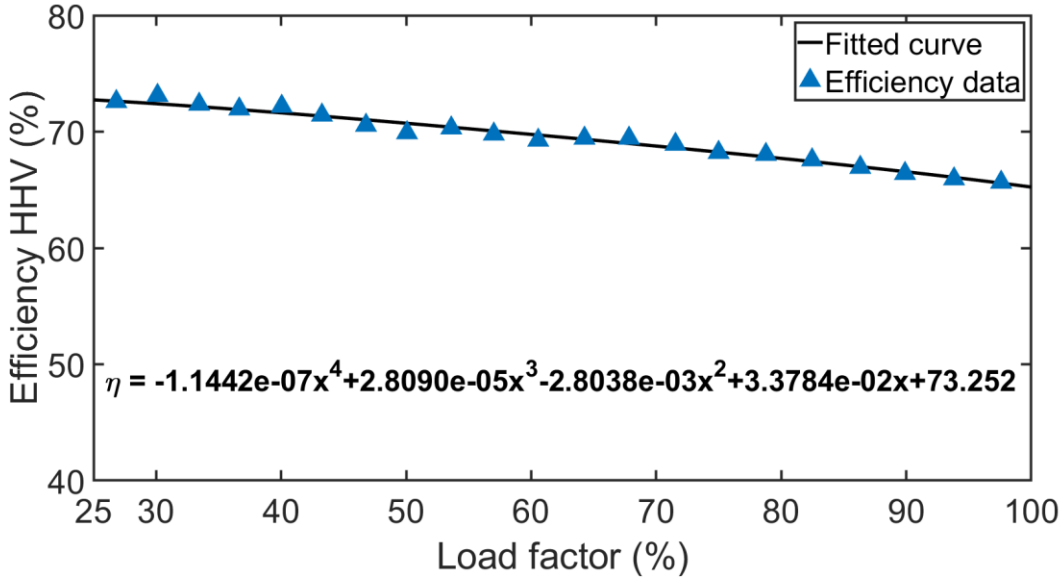

Figure 5 - Part load electrolyzer system efficiency on the load range, adapted from [34]

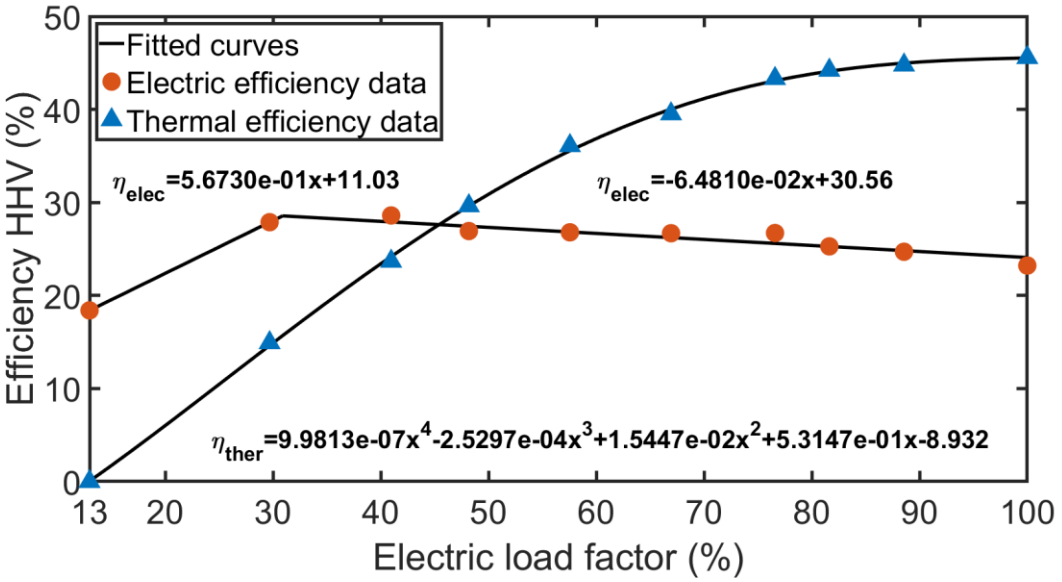

Figure 6 – Part load fuel cell system efficiency the load range, adapted from [32]

2.2.3. Strategies

At the system level, habitations prioritize self-consumption. Consequently, energy generated by photovoltaic panels is initially allocated to meet the buildings' requirements. If there is surplus energy, the storage loop (comprising the electrolyzer and battery) comes into play to store the excess. Conversely, if production falls short, the destocking loop (involving the fuel cell and battery) intervenes. In case of excessive demand, electricity from the national electrical network supplements the shortfall.

At the component level, the system requires rules to determine which component absorbs or provides energy at a given moment. While the study does not necessitate a formal control system, operational strategies need to be established.

An essential decision involves choosing whether the fuel cells address electrical or thermal needs first. Typically, combined heat and power systems (CHP) prioritize heat demand. However, research by Romdhane and Louahlia-Gualous suggests that, for PEMFC, an electrically led system yields better economic results [41]. Thus, this approach is adopted, leading to instances where the fuel cell produces heat when it may not be immediately needed. This heat is sent to the buildings' hot water storage if their temperature is not already too high and discarded otherwise.

Another consideration is determining which component (fuel cells, electrolyzer, and battery) responds first when energy is needed or provided. Based on the results of Monforti et al., a battery priority strategy is chosen, as the results indicate that it yields better economic results for a battery and hydrogen system providing electricity to a building [43].

For the destocking part, a battery priority approach is employed based on these results but also to solicit the fuel cell for shorter duration. This strategy also facilitates using the fuel cells at power closer to nominal by recharging the battery simultaneously, as providing energy to the building which contributing to better fuel cell aging [36].

To maintain consistency, the stocking operating strategy also prioritizes the battery over the electrolyzer. In this case, the electrolyzer only activates once the battery has reached a sufficiently high state of charge (SOC).

The chosen strategy flow chart is shown in Fig. 7. Generally, the system operates by testing component availability. If multiple systems are available, the battery takes priority. If one system alone cannot absorb or provide the required power, others assist if possible. In cases where needs cannot be entirely met, the remaining energy is provided by the grid. Conversely, if energy cannot be fully absorbed, surplus electricity is assumed to be discarded into the grid, with the amount discarded varying depending on component sizes.

The system deviates from this functioning in two cases to mitigate hydrogen system dynamics. Firstly, when the battery is nearly fully charged (>85%), half of the electricity is shared with the electrolyzer to facilitate a smoother transition/start-up. Secondly, when the fuel cell is already operational, it continues running until the battery is almost full (>80%) to reduce the frequency of fuel cell ON/OFF transitions.

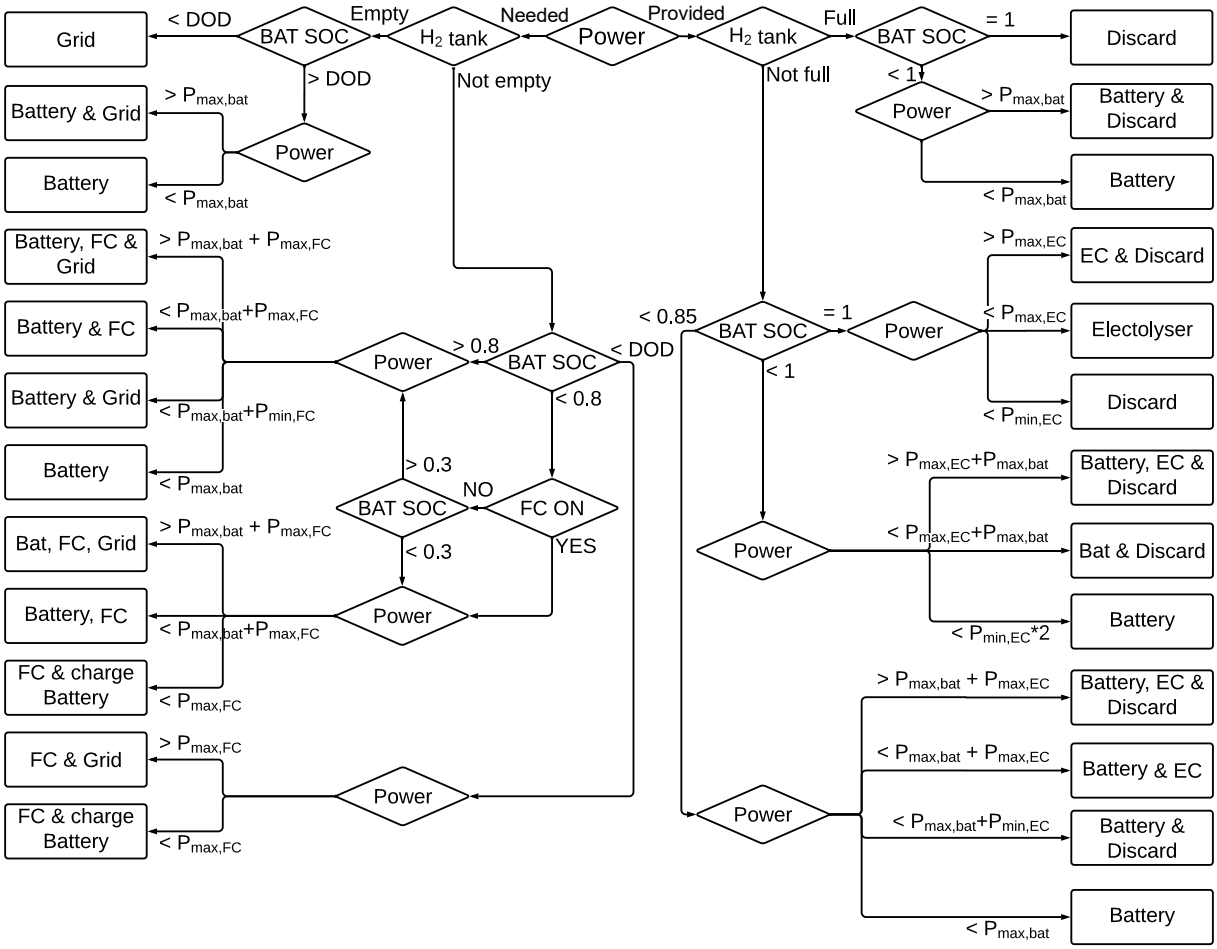

Figure 7. Flow chart of the operation strategies

2.3. Optimization

The optimization involves 5 variables (fuel cell power, electrolyzer power, tank size, battery size, and PV area) and 2 objectives: cost and greenhouse gas emissions. For a given configuration, performance testing is conducted over one year. Simulations start on the 15th of April, considered as the end of the heating season, corresponding to a time when the hydrogen tank is at its minimum (no storing between years is considered). The cost and emission performances of the system are estimated using the following methodology.

2.3.1. Cost objective

Table 3 – Cost optimization parameters

System	Investment[a]	Lifetime	O&M (per year)	Ref.
Electrolyzer (PEM)	1523€/kW	20 years	3% investment	[44, 39]
Fuel cells (PEM)	2500€/kW	10 years	3% investment	[37, 39]
Hydrogen tank	690€/kg_{H2}	20 years	3% investment	[45, 39]

Battery (Li-on)	550€/kWh	10 years	0% investment	[39]
PV (monocrystalline)	1670€/kWp	20 years	3% investment	[39]
DC/DC converter[b]	900€/kW	33 years	3% investment	[39]
Electricity cost	0.221€/kWh			[46]

a: Cost converted to euros and with inflation included for oldest values
b: Only for the fuel cells because all other power electronics are included in their respective system price

For economic performance, on one side, the calculation is needed to determine the cost of a given configuration of the systems. Eq. 11 calculates the capital expenditure (CAPEX) as the sum of the initial investment of all systems considered and the sum of all replacement costs. Additional costs are considered for all systems with lifetimes less than 20 years (fuel cells and battery). Those replacement costs are equal to the investment cost times the number of replacements needed for a global system lifetime of 20 years.

Eq. 12 calculates the operating expenditure (OPEX) as the sum of the yearly operation and maintenance cost (O&M) for the global system lifetime (20 years). By adding the CAPEX and the OPEX, the total cost of the system for its lifetime is obtained (Eq. 13). In this economic analysis, parameters such as the interest rate, inflation rate, tax credit are neglected.

On the other side, expression of the economic gain that a configuration creates by providing the buildings with electricity and heat is needed. For that goal, heat and electricity balances are expressed for all buildings at each time step. First for the heat side, only the fuel cells provide direct thermal energy. The power deficit is thus the result of the power balance between the 100 buildings' needs (space and water heating) and the fuel cell production (Eq. 14). If there is still a need for heat in the buildings, the heat pumps will have to provide the rest and thus increase the electric load. On the contrary, if there is too much heat produced, this heat will be absorbed in the hot water tanks if possible or discarded if not (Eq. 15). The useful heat provided is thus the difference between the yearly production of the fuel cells and this discarded heat (Eq. 16).

Then for the electricity part, all the components of the system intervene (photovoltaics panels, electrolyzer, fuel cells, and battery). The buildings' electrical demand is composed of the power consumption of appliances, lighting, cooling, and the heating electrical load previously calculated (Eq. 17). The demand is compared to the production/absorption of the 4 components to obtain the electricity deficit (Eq. 18). Only when the system cannot completely address the building demands is the electric network called to provide the rest (Eq. 19). On the other hand, if there is too much production, the electricity is discarded. The electric energy directly provided by the system is then obtained with the difference between the building electricity demand and the energy provided by the electrical network (Eq. 20).

Finally, these calculations are used to estimate how much saving the system provides. Because the buildings' heating systems use electricity, both gains correspond ultimately to electricity gains. Thermal and electric gains are thus grouped into electricity gain using the heating systems' parameters (Eq. 21). Then, these electricity gains are transformed into economic gains with the electricity tariff, assuming that for the 20 years of its lifetime, the system will provide the same electricity gain each year (Eq. 22).

In the end, both electric and thermal energies are combined in Eq. 23 to obtain the system's economic performance with the difference between the total cost and the economy saving estimated for the 20 years of its lifetime. Table 3 gathers all the parameters used in these equations.

The values originate from literature articles and reports from international agencies. They are in accordance with the ranges defined by international agencies and reported in [47]. The cost of the urban heat network is not considered. The fuel cell cogeneration produces only a small fraction of the buildings' heating needs. An actual heat network would serve as a carrier for a larger heat quantity provided by a myriad of other possible heat sources: natural gas, biogas, waste incineration, industrial heat recovery… This is thus considered as already present.

$$CAPEX = \sum_{systems} C_{inv,sys} + \sum_{systems} C_{rep,sys} \tag{11}$$

$$OPEX = Lifetime * \sum_{sytems} C_{O\&M,sys} \tag{12}$$

$$C_{total} = OPEX + CAPEX \tag{13}$$

$$P_{deficit,ther} = P_{hot\_water} + P_{space\_heating} - P_{FC,ther} \tag{14}$$

$$P_{deficit,ther} \begin{cases} \geq 0 \rightarrow P_{discard,ther} = 0 \,;\, P_{heating,elec} = P_{deficit,ther} \,/\, COP_{hp} \\ < 0 \rightarrow -P_{deficit,ther} \begin{cases} > P_{absorb,hw} \rightarrow P_{discard,ther} = -P_{deficit,ther} - P_{absorbable} \\ < P_{absorb,hw} \rightarrow P_{discard,ther} = 0 \end{cases} \end{cases} \tag{15}$$

$$H_{prov} = (P_{FC,ther} - P_{discard,ther}) * \Delta t \tag{16}$$

$$P_{demand,elec} = P_{appliances} + P_{lighting} + P_{cooling} + P_{heating,elec} \tag{17}$$

$$P_{deficit,elec} = P_{demand,elec} + P_{bat,charge} + P_{EC} - P_{PV} - P_{FC,elec} - P_{bat,discharge} \tag{18}$$

$$P_{deficit,elec} \begin{cases} > 0 \rightarrow P_{grid,elec} = P_{deficit,elec} \\ < 0 \rightarrow P_{grid,elec} = 0 \,;\, P_{discard,elec} = -P_{deficit,elec} \end{cases} \tag{19}$$

$$E_{prov,direct} = (P_{demand,elec} - P_{grid,elec}) * \Delta t \tag{20}$$

$$E_{prov,total} = \sum_{year} (E_{prov,direct} + H_{prov} \,/\, COP_{hp}) \tag{21}$$

$$G_{cost} = (E_{prov,total} * E_{tariff}) * Lifetime \tag{22}$$

$$Obj_{cost} = C_{total} - G_{cost} \tag{23}$$

2.3.2. Carbon emission objective

Table 4 – Carbon emissions optimization parameters

System	Carbon intensity	Ref.
Electrolyzer (PEM)	29.4 $kgCO_2$-eq/kW	[48]
Fuel cells (PEM)	30 $kgCO_2$-eq/kW	[49]
Hydrogen tank	200 $kgCO_2$-eq/kg_{H2}	[50]
Battery (Li-on)	137.34 $kgCO_2$-eq/kWh	[51]
PV (monocrystalline)	2113 $kgCO_2$-eq/kWp	[52]
Electricity average	0.247 $kgCO_2$-eq kWh	[53]

The emission analysis follows a similar approach as in the cost analysis. Utilizing the parameters in Table 4, the system's life cycle impact on greenhouse gases is calculated, considering the individual components' impacts and the impact of component replacement necessary for a 20-year lifetime (Eq. 24).

Life cycle assessments are less common than cost analysis, which makes the data for life cycle emissions scarcer than cost data, especially for hydrogen systems, and the data collection more challenging. Therefore, values from sources using different calculation methodologies are employed.

For assessing the emission reduction of the system, the total energy provided by the system is utilized (Eq. 25). This time, instead of a fixed rate, the carbon intensity of the electrical grid will vary throug h each hour of the year based on the data from the British grid [37]. Finally, the system's performance regarding greenhouse emissions is obtained by the difference between the life cycle emissions of the systems and the emissions it prevents (Eq. 26).

$$Em_{total,sys} = \sum_{sytems} Em_{inv,sys} + \sum_{sytems} Em_{rep,sys} \tag{24}$$

$$Em_{prevented} = Lifetime * \sum_{year} (E_{prov,total} * Em_{elec}) \tag{25}$$

$$Obj_{emission} = Em_{total,sys} - Em_{prevented} \tag{26}$$

2.3.3. Multi-objective optimization technique

To create the optimization setup, all the model's components are calculated independently from the hydrogen systems (Climate, PV, appliances, lighting, cooling…). This allows for faster computing and isolates all the stochastic parts of the CREST model outside of the optimization.

For the optimization itself, two mono-objective optimizations are initially performed to identify the best relative configuration. Due to the high resolution (1 minute) and the duration of the simulation (1 year), the objective function is time-consuming. Hence, the MATLAB surrogate optimization tool is utilized. This algorithm uses a surrogate of the objective function constructed by a radial basis function. The surrogate minimizes the required number of function evaluations, which is crucial for time-consuming objective functions [54].

Subsequently, these relative optimums serve as starting points for the MATLAB multi-objective elitist genetic algorithm to obtain the Pareto front. To achieve a more comprehensive Pareto front, dominant points are extracted from all generations rather than just the last one. If there are still clear non-optimal configurations, such as those with one hydrogen component but not the others, those points are reevaluated without all hydrogen components.

3. Results and discussion

In this section, the results of the optimization are presented, displaying the population output of the genetic algorithm and comparing those results to the literature.

3.1. Pareto front

The results of the multi-objective optimization are shown in Fig. 8 in the form of a Pareto front. The x-axis represents the cost remaining after 20 years. A negative economic impact means that the system brings an economic gain compared to using grid electricity. The y-axis represents the amount of CO_2 equivalent the system will create for its entire life cycle. A negative impact means the system will avoid more emissions than it will create. Each point on the graph represents a dominant configuration.

The figure also contains a comparison to a Pareto front created using a direct multisearch optimization algorithm. This second algorithm gives similar results but does not capture the full range of the Pareto front, especially on the CO_2 side, ignoring all configurations using hydrogen systems. Only the genetic algorithm results are presented in the following sections.

The economic performances of the systems after 20 years, compared to simply using the electricity grid, range between a gain of 304 k€ and an over cost of 1.42 million euros. For the emission side, all the configurations bring an emission reduction, with performances ranging between 555 and 1284 tonnes of CO_2 equivalent. This highlights the high carbon intensity of the UK grid compared to what can be locally produced by PV power independently of the energy storage configuration. On the other hand, not all configurations bring economic gains, illustrating the importance of carefully sizing this type of district-sized systems.

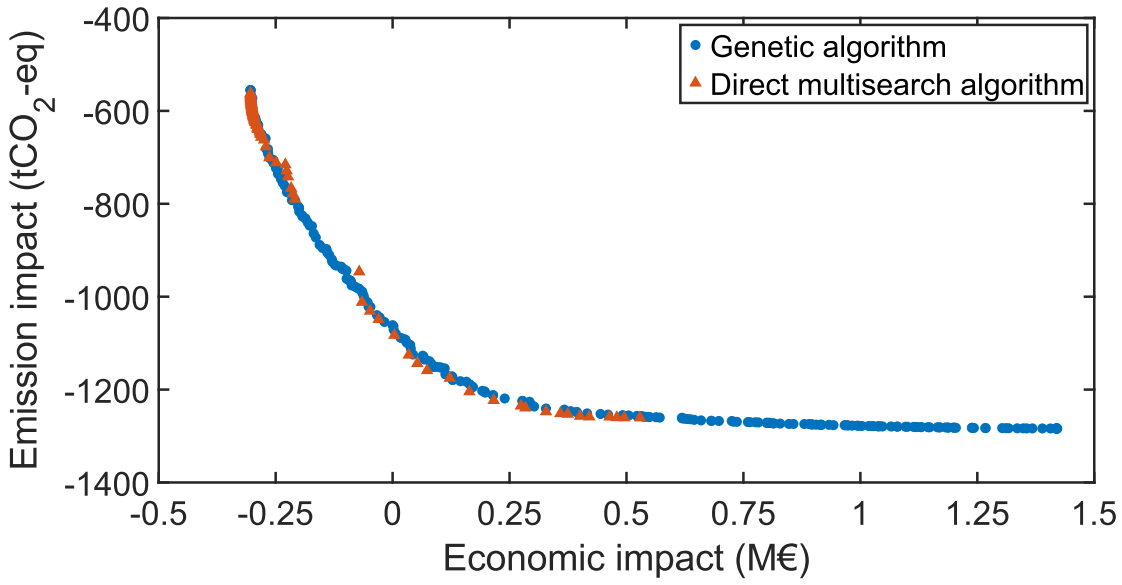

Figure 8. Pareto front

3.2. Mono objective optimums

3.2.1. Economic optimum

The optimal economic solution consists only of a 35.44 kWh battery and 1120 m² of PV panels shared among the habitations (Table 5). This configuration, after 20 years, corresponds to a total investment of 545 k€ and provides electricity savings equivalent to 42.4 k€ per year. Thus, it brings an estimated economic gain of 304 k€ after 20 years. This system also allows for a non-negligible emission reduction of 555 tonnes after 20 years by locally producing around 23.2% of the buildings' energy needs.

The configuration's operation during a typical week is illustrated in Fig. 9. The graph represents the net demand, where a positive net demand indicates that the buildings need energy, and a negative one means the PV production exceeds the demand. For this configuration, only the battery and the grid respond to the demand side, and only the battery absorbs the overproduction side.

The PV size provides enough electricity to meet the energy needs only during periods of significant irradiation. Hence, during the summer and transition seasons (fall and spring), the PV covers daytime needs, while the battery balances the system when irradiation decreases during the daytime or, on the sunniest day, provides energy in the early evening. Conversely, during winter, the buildings absorb all the PV electricity, but it is insufficient to meet their needs, leaving the battery mostly empty.

Overall, this very small system only meets the demand for a few hours during the daytimes. These results indicate that PV panels can compete with UK grid prices even without storage options. However, the storage options do not compete and are thus reduced by the optimization to smaller sizes compared to the nighttime needs.

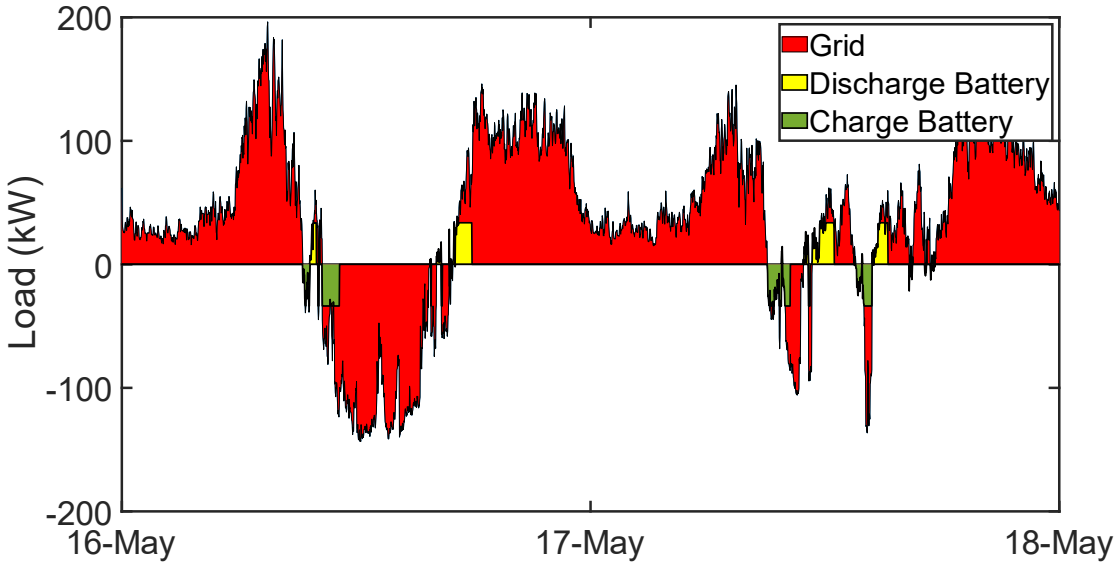

Figure 9. Power balance for cost optimum in May

3.2.2. Emission optimum

On the emission side, the optimal solution consists of a 40 kW fuel cell, a 285 kW electrolyzer, 43.3 kg of dihydrogen storage, a 1133 kWh battery, and 3435 m² of PV (Table 5). This configuration allows, compared to total grid usage, for an emission reduction of 1284 tonnes after 20 years, which

corresponds to local production of around 66.5% of the buildings' energy needs. It also corresponds, after 20 years, to a total investment of 3855 k€ and brings an electricity economy equivalent to 122 k€ per year. Thus, resulting in an estimated over cost of 1421 k€ after 20 years. Together, this means a price of 1107 euros per tonne of CO_2 equivalent.

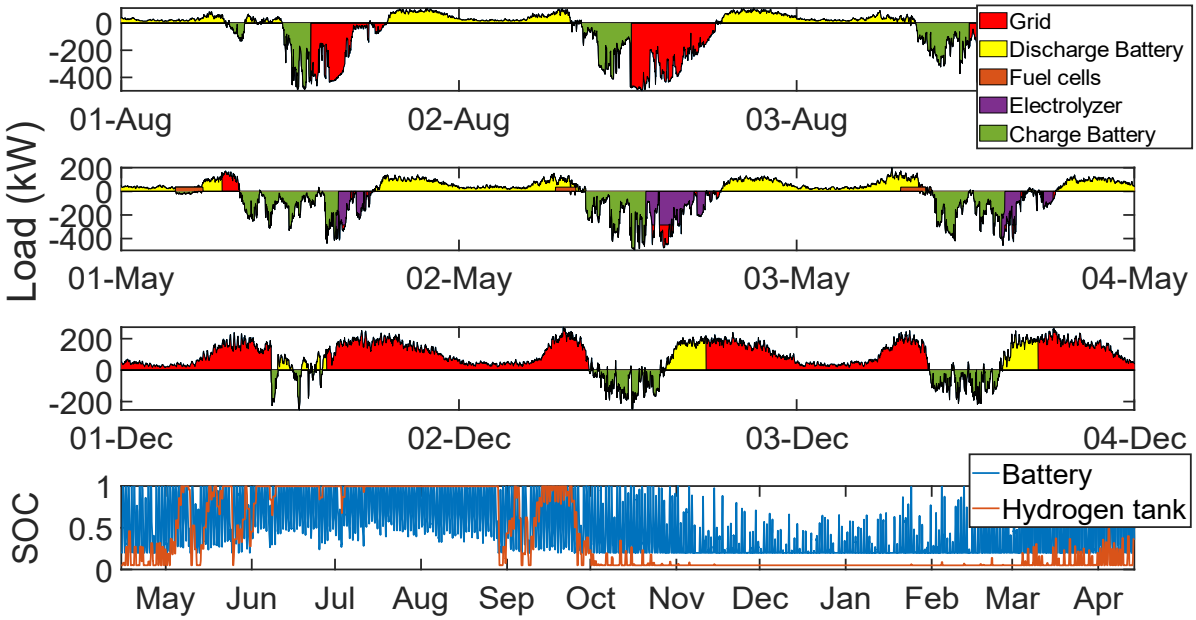

Figure 10. Power balance for emission optimum in a typical week

Fig. 10 illustrates the power balance for the emission optimum for three typical periods and the tank and battery evolution throughout the year. This configuration has a larger PV size than the cost optimum, leading to higher overproduction during daytimes. This overproduction is not significant enough in winter to completely charge the battery, so the system only meets a fraction of the nighttime demand. In summer, the longer daytime and lower demand allow the battery to fully charge and meet the nighttime demand. The hydrogen systems are thus only utilized during the transitional seasons when they act as supplementary storage capacity.

Overall, this indicates that the storage option competes with the grid, emission-wise, for meeting electricity and hot water loads. However, none of the storage options (battery and hydrogen) compete for the winter space heating load. This includes the fuel cell, even though it produces heat directly by cogeneration. It may be due to the amount of losses in the thermal loop, especially in the district heat network.

Throughout the year, the system provides 65% of the district's electricity and heat needs. This means that replacing more of the grid electricity, either by increasing energy storage (battery, hydrogen tank, battery) or the system's output power (PV, fuel cell, battery), is not environmentally interesting in terms of life cycle emissions.

3.2.3. Medium cost optimum

The entire set falls between these two optima. The closer a configuration is to the cost optimum, the smaller its components are; conversely, the closer it is to the emission optimum, the larger the components become. An interesting point between the two optima is the medium-cost point, namely the point in the middle between the most and least expensive configurations, as at that point, more than 90% of the emission reduction potential is already achieved.

In the Pareto front, this point represents a configuration with a 10.3 kW fuel cell, a 49.6 kW electrolyzer, 21.5 kg of dihydrogen storage, a 1103 kWh battery, and 3204 m² of PV (Table 5). It caters to around 63% of the building's needs. This configuration is similar to the emission optimum but scaled down. Thus, the net cost of the system is much lower at around 563 k€ and performs only slightly worse on the emissions side, around 1260 tonnes of CO_2 equivalent (98% of the emission optimum). This results in a cost of 447 euros per tonne of CO_2 equivalent.

It is noteworthy that even though the sizes of the components differ significantly from the emission optimum, the difference in emission gain is rather small. This is due to the fact that the easiest part of the load is already met (sunniest day, day without heating, etc.). Thus, even for a small increase in the proportion of the energy provided by the system, a substantial investment is necessary. This configuration offers a trade-off between the two criteria but is still rather expensive, like all configurations with significant hydrogen system sizes. On the other hand, configurations using only PV and battery achieve good economic performances but are not able to achieve high emission gains, mostly because solar gains are small in winter, and a bigger battery storage leads to more CO_2 life cycle emissions.

Table 5 – Cost optimization parameters

System	**Cost optimum**	**50 % cost**	**Emission optimum**
Fuel cells (PEM)	0 kW	10.3 kW	39.7 kW
Electrolyzer (PEM)	0 kW	49.6 kW	285.1 kW
Hydrogen tank	0 kg_{H2}	21.5 kg_{H2}	43.3 kg_{H2}
Battery (Li-on)	35.44 kWh	1103 kWh	1133 kWh
PV (monocrystalline)	1120 m^2	3204 m^2	3435 m^2
Economic performances	-304 k€	563 k€	1421 k€
Emission performances	-555 tCO_2-eq	-1260 tCO_2-eq	-1284 tCO_2-eq

3.3. Population composition

3.3.1. Components' sizes

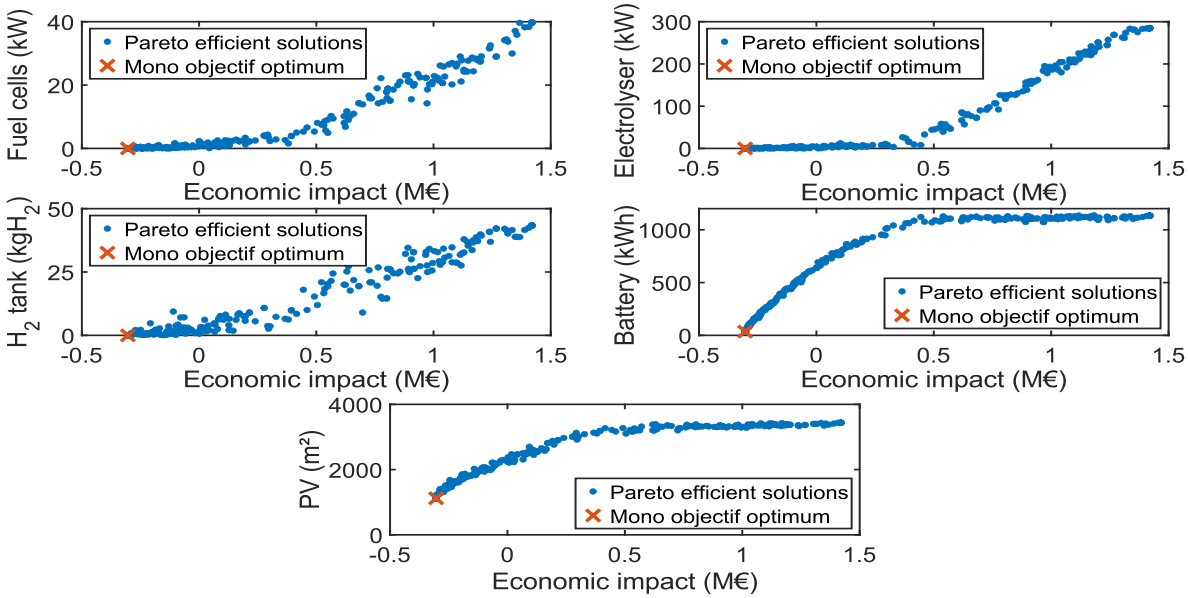

Figure 11. Economic performances in regard to the optimization variables (components sizes)

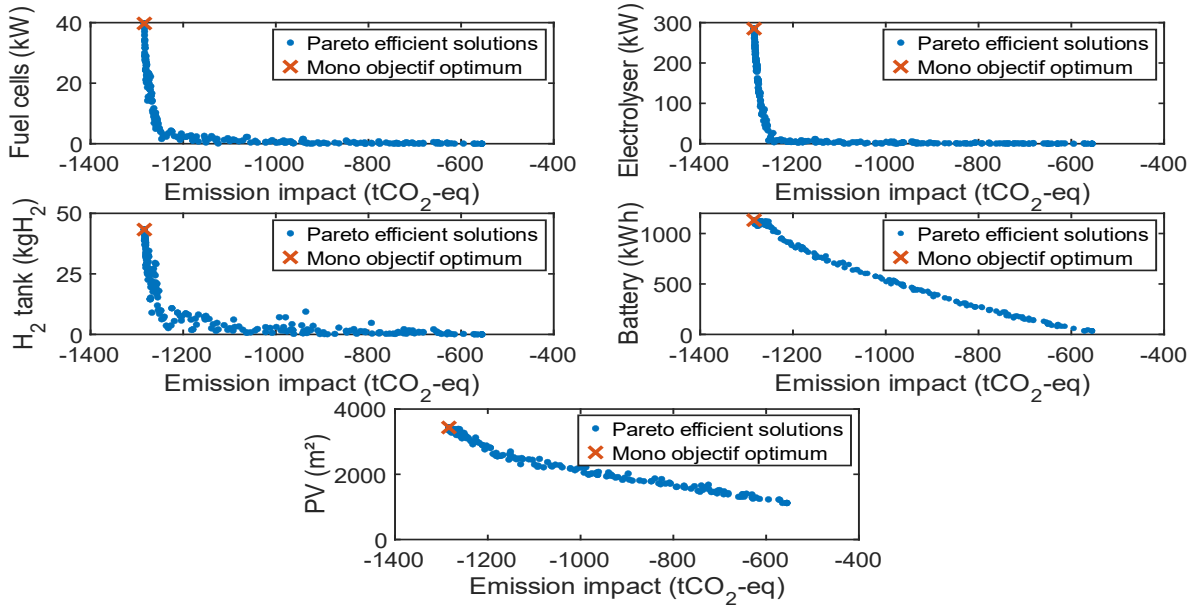

Figure 12. Emission performances in regard to the optimization variables (components sizes)

Fig. 11 and 12 show the economic and emission performances, respectively, depending on the size of the system components for all dominant solutions found. The results are highly specific to factors such as building types, climate, and heating system usage, among others. However, trends can be discerned from them.

On the economic side, an increase in the size of the components related to the hydrogen loop (fuel cells, electrolyzer, and hydrogen tank) translates to a decrease in economic interest. For the battery and PV, the results converge around the values presented above. Configurations with sizes below are

non-Pareto efficient, and sizes above are less economically interesting. Overall, both energy storage options do not perform well economically, and direct PV usage is almost the exclusive energy source for the best-performing configurations cost-wise.

In terms of emission performances, an increase in the size of the fuel cells and the electrolyzer strongly improves performances until a value around 10 kW and 100 kW, respectively, after which it only improves marginally. The cutting point is less clear in the hydrogen tank case, but configurations with a tank size between 15 and 45 kg of dihydrogen seem to bring similar emission performances. For the PV and battery, the performances decrease faster until the values presented in the emission optimum values above do not bring better performances in the economic and emission size.

The value of using life cycle emission analysis instead of optimizing only on the emission during operation is evident here. The component sizes increase until arriving at a balance between the system emission in its early and end of life and the emission reduction during operation, at which point the emission performances stop improving. On the other hand, in an operation emission optimization, the system sizes would increase until most of the carbonate grid electricity is replaced by locally produced energy, disregarding the negative environmental impact that producing and dismantling such a large system would bring. This balance is linked to the UK electricity grid emission intensity and would drastically change from one energy mix to another, like if another country's electricity grid is considered or if fossil fuel (gas, diesel, etc.) is used for heating.

3.3.2. Cost of energy

Cost of energy is an economic criterion widely used in the literature. However, it is an index that can provide an incomplete view of cost performances because it does not necessarily reflect the quantity of energy provided by the system. In an off-grid design or a design with an autonomy goal, the energy quantity provided is already constrained. But it would not be the case here. Thus, the energy provided by the grid is also included in the cost of energy.

The cost of energy, including energy provided by the system and by the grid, ranges in the study from 0.203 €/kWh for the cost optimum to 0.307 €/kWh for the emission optimum. The prices of energy vary significantly depending on the type of components used in the study, technology data used, size of the demand, economic assumptions made, electricity rates, etc.

Comparing the results with two multi-optimization study presented in the introduction. Gabrielli et al. find, for the cost optimum, an average cost of energy of 0.07 €/kWh and, for the emission relative optimums, an average cost of energy of 0.5 €/kWh [13, 14]. Compared to the results, a lower floor for costs of energy is observed. This is due to the use of configurations with a gas boiler, whereas heat pumps are used as the default option and the use of gas boilers is discarded, bringing a higher cost of energy floor.

Arsalis et al. conduct a technoeconomic analysis of a PV/EC/FC system [12]. The selected configuration consists of a 584 kW electrolyzer, a 92 kW fuel cell, and a 21-ton hydrogen storage unit The resulting cost of energy is 0.216 €/kWh. This cost is notably lower than the figure calculated, in the present study, for systems utilizing hydrogen components. The variance arises from the comprehensive economic analysis conducted, encompassing cost reductions such as capital depreciation, tax credits, loan interest deductions, and salvage value. The combination of these four cost reductions reduces the effective life cycle cost of the system to approximately 35% of the total system cost, thereby significantly lowering the cost of energy.

3.3.3. Systems structures

Overall, looking at both objectives, several observations can be made. Beyond 35 m² of PV per house, performances decrease in terms of both cost and emission because it generates excess electricity, and storage options are not competitive. Fuel cell sizes are almost always smaller than electrolyzer sizes by a ratio close to 6.3 (for fuel cell sizes above 1 kW). Seasonal storage does not perform well with both criteria, and only configurations with no or relatively small hydrogen storage appear in the Pareto set. In this specific case study, the best use for hydrogen systems is to serve as a balance during transitional seasons, not to store energy to meet winter demand. With the considered parameters, neither hydrogen nor battery storage options have good enough life cycle emission performances to provide environmentally relevant seasonal storage.

Thus, none of the configurations in the Pareto front can completely meet the high winter load created by the increase in space heating needs. This means that the component sizes necessary to address the space heating needs all year long do not provide enough economic and emission gains to compensate for their life cycle cost or emissions. This result heavily depends on the comparison of the system performances to heat pumps, which answer the heating load more efficiently than gas boilers.

Even in configurations with the largest fuel cells, no heat is discarded throughout the year. The optimization algorithm reduces discarded heat, suggesting that fuel cell-based system performances are only interesting if all the produced heat can be used directly or stored. Since centralized thermal storage is not considered, the heat storable is dependent on the size of the houses' hot water storages and cannot adapt to larger fuel cell sizes. Testing configurations considering centralized heat storage could be interesting.

Comparing the systems structures with a multi-optimization study presented in the introduction Gabrielli et al. find a cost relative optimum that uses only a heat pump, a gas boiler, and centralized heat storage, and an emission optimum that uses a heat pump working with a PV/EC/FC/Bat system and centralized heat storage [13, 14]. Gabrielli et al. reach similar results as the present study on the hydrogen systems being useful for emissions reduction but not for cost economies. However, the size of the hydrogen systems used for the emission optimum is superior to the ones found in the present study. This difference may be due to not considering the use of centralized heat storage and only storing heat in limited capacity inside the houses' hot water storages. With a smaller heat storage capacity, the benefit of a cogeneration system decreases.

In contrast to the present results, Gabrielli et al. find interest in using seasonal hydrogen storage regarding the operation emission criteria. This highlights the different design philosophy between using only operation emissions and using whole life cycle emissions as in the present paper. Optimizing on the complete life cycle emission will penalize larger hydrogen tanks necessary for seasonal storage: a larger tank will allow the systems to avoid more emission during operation but will also cause more emissions related to material extraction, assembly, transport...

Naumann et al. observed that in the life cycle analysis of residential hydrogen-based energy storage, the production of hydrogen tanks is the primary source of emissions [25]. The multi-objective optimization presented here confirms this and goes further, demonstrating that this substantial life cycle impact plays a pivotal role in the future environmental viability of hydrogen-based seasonal storage systems.

4. Conclusion

The goal of the present work is to model and optimize the cost and greenhouse gas emissions of a residential district multi-energy system to highlight sizing rules. For this purpose, a widely used residential load model was re-implemented and modified to produce a district load composed of an aggregation of 100 single-family houses loads. A grid-connected multi-energy system, consisting of PV panels, a battery, an electrolyzer, a hydrogen tank, and a fuel cell, interacts with the load simulation and addresses the district's heat and electricity needs.

The multi-objective optimization creates a set of dominant configurations. In this set, all configurations result in an emission reduction compared to complete grid reliance. This means that a large set of different PV/EC/FC/battery configurations can compete with the grid in terms of emissions. However, only configurations based solely on PV and battery are cost-efficient. Thus, adding hydrogen systems improves emission performance but worsens cost performance. Overall, the present sizes of hydrogen systems depend mostly on how much emphasis is put on reducing greenhouse emissions. An interesting configuration is composed of 32 m² of PV per house, a 10 kW fuel cell, a 50 kW electrolyzer, 21.5 kg of hydrogen storage, and 1100 kWh of battery storage. It can provide around 63% of building needs, bringing an emission gain of 1284 tonnes of CO_2 equivalent after 20 years.

Optimizing based on system cost and life cycle greenhouse gas emissions underlines noteworthy sizing principles. Firstly, it shows that providing the total energy demand is not pertinent in this grid-connected case, given the significant life cycle emissions impact of the systems that would be required compared to the grid carbon intensity. The best-performing configuration on the economic side provides around 23% of the total energy and around 65% for the emission side. Locally producing the other 35% does not seem relevant compared to the considered base energy sources (all electricity and heating needs met by the UK electricity grid). Life cycle emission analysis also highlights that none of the storage options (battery and hydrogen) show good prospects for seasonal energy storage. The analysis identifies hydrogen tank life cycle emissions as a major bottleneck for the relevance of seasonal hydrogen storage in enhancing residential sustainability. Therefore, the future of seasonal hydrogen storage is highly linked to the tank manufacturing emissions and the means of recycling materials used.

Declaration of competing interest

The authors declare that they have no known competing financial interests or personal relationships that could have appeared to influence the work reported in this paper.

Acknowledgments

This work has been supported by the EIPHI Graduate School (contract ANR-17-EURE-0002) and the Region Bourgogne Franche-Comté.

Computations have been performed on the supercomputer facilities of the Mésocentre de calcul de Franche-Comté

5. Bibliographie

[1] H. Q. Nguyen, A. M. Aris et B. Shabani, «PEM fuel cell heat recovery for preheating inlet air in standalone solar-hydrogen systems for telecommunication applications: An exergy analysis,» *International Journal of Hydrogen Energy,* vol. 41, p. 2987–3003, 2016.

[2] P. Zhao, J. Wang, L. Gao et Y. Dai, «Parametric analysis of a hybrid power system using organic Rankine cycle to recover waste heat from proton exchange membrane fuel cell,» *International Journal of Hydrogen Energy,* vol. 37, p. 3382–3391, 2012.

[3] Y. Qin, H. Zhang et X. Zhang, «Integrating high-temperature proton exchange membrane fuel cell with duplex thermoelectric cooler for electricity and cooling cogeneration,» *International Journal of Hydrogen Energy,* vol. 47, pp. 38703-38720, 2022.

[4] F. Musharavati et S. Khanmohammadi, «Performance improvement of a heat recovery system combined with fuel cell and thermoelectric generator: 4E analysis,» *International Journal of Hydrogen Energy,* vol. 47, pp. 26701-26714, 2022.

[5] H. Tao, K. A. Mamun, A. Ali, E. Solomin, J. Zhou et N. Sinaga, «Performance enhancement of integrated energy system using a PEM fuel cell and thermoelectric generator,» *International Journal of Hydrogen Energy,* 2023.

[6] S. Ham, D. Park, W.-Y. Lee et M. Kim, «Simulation to analyze operation strategy of combined cooling and power system using a high-temperature polymer electrolyte fuel cell for data centers,» *International Journal of Hydrogen Energy,* vol. 48, pp. 8247-8259, 2023.

[7] H. Lambert, R. Roche, S. Jemeï, P. Ortega et D. Hissel, «Combined Cooling and Power Management Strategy for a Standalone House Using Hydrogen and Solar Energy,» *Hydrogen,* vol. 2, p. 207–224, 2021.

[8] F. Tooryan, H. HassanzadehFard, V. Dargahi et S. Jin, «A cost-effective approach for optimal energy management of a hybrid CCHP microgrid with different hydrogen production considering load growth analysis,» *International Journal of Hydrogen Energy,* vol. 47, pp. 6569-6585, 2022.

[9] A. Maleki, H. Hafeznia, M. A. Rosen et F. Pourfayaz, «Optimization of a grid-connected hybrid solar-wind-hydrogen CHP system for residential applications by efficient metaheuristic approaches,» *Applied Thermal Engineering,* vol. 123, p. 1263–1277, 2017.

[10] H. Chang, X. Xu, J. Shen, S. Shu et Z. Tu, «Performance analysis of a micro-combined heating and power system with PEM fuel cell as a prime mover for a typical household in North China,» *International Journal of Hydrogen Energy,* vol. 44, p. 24965–24976, 2019.

[11] M. Hosseini, I. Dincer et M. A. Rosen, «Hybrid solar-fuel cell combined heat and power systems for residential applications: Energy and exergy analyses,» *Journal of Power Sources,* vol. 221, p. 372–380, 2013.

[12] A. Arsalis, A. N. Alexandrou et G. E. Georghiou, «Thermoeconomic modeling of a completely autonomous, zero-emission photovoltaic system with hydrogen storage for residential applications,» *Renewable Energy,* vol. 126, p. 354–369, 2018.

[13] P. Gabrielli, F. Fürer, G. Mavromatidis et M. Mazzotti, «Robust and optimal design of multi-energy systems with seasonal storage through uncertainty analysis,» *Applied Energy,* vol. 238, pp. 1192-1210, 2019.

[14] P. Gabrielli, M. Gazzani, E. Martelli et M. Mazzotti, «Optimal design of multi-energy systems with seasonal storage,» *Applied Energy,* vol. 219, pp. 408-424, 2018.

[15] C. Ghenai et M. Bettayeb, «Modelling and performance analysis of a stand-alone hybrid solar PV/Fuel Cell/Diesel Generator power system for university building,» *Energy,* vol. 171, p. 180–189, 2019.

[16] M. Kilic et A. F. Altun, «Dynamic modelling and multi-objective optimization of off-grid hybrid energy systems by using battery or hydrogen storage for different climates,» *International Journal of Hydrogen Energy,* vol. 48, pp. 22834-22854, 2023.

[17] R. S. El-Emam, M. F. Ezzat et F. Khalid, «Assessment of hydrogen as a potential energy storage for urban areas' PV-assisted energy systems - Case study,» *International Journal of Hydrogen Energy,* vol. 47, pp. 26209-26222, 2022.

[18] Q. Guo, Y. Chen, Y. Xu, S. Nojavan, H. Bagherzadeh et E. Valipour, «Integration of hydrogen storage system and solar panels in smart buildings,» *International Journal of Hydrogen Energy,* vol. 47, pp. 19237-19251, 2022.

[19] O. M. Babatunde, J. L. Munda et Y. Hamam, «Hybridized off-grid fuel cell/wind/solar PV /battery for energy generation in a small household: A multi-criteria perspective,» *International Journal of Hydrogen Energy,* vol. 47, pp. 6437-6452, 2022.

[20] A. Mohammed, A. M. Ghaithan, A. Al-Hanbali et A. M. Attia, «A multi-objective optimization model based on mixed integer linear programming for sizing a hybrid PV-hydrogen storage system,» *International Journal of Hydrogen Energy,* vol. 48, pp. 9748-9761, 2023.

[21] J. Mustafa, S. Alqaed, F. A. Almehmadi, E. H. Malekshah et M. Sharifpur, «Effect of economic and environmental parameters on multi-generation of electricity, water, heat, and hydrogen in Saudi Arabia: A case study,» *International Journal of Hydrogen Energy,* 2023.

[22] I. U. Diaz, W. de Queiróz Lamas et R. C. Lotero, «Development of an optimization model for the feasibility analysis of hydrogen application as energy storage system in microgrids,» *International Journal of Hydrogen Energy,* vol. 48, pp. 16159-16175, 2023.

[23] M. M. Samy, S. Barakat et H. S. Ramadan, «A flower pollination optimization algorithm for an off-grid PV-Fuel cell hybrid renewable system,» *International Journal of Hydrogen Energy,* vol. 44, pp. 2141-2152, 2019.

[24] D. C. Šanić et F. Barbir, «Stand-alone micro-trigeneration system coupling electrolyzer, fuel cell, and heat pump with renewables,» *International Journal of Hydrogen Energy,* vol. 47, pp. 35068-35080, 2022.

[25] G. Naumann, E. Schropp, N. Steegmann, M. C. Möller et M. Gaderer, «Environmental performance of a hybrid solar-hydrogen energy system for buildings,» *International Journal of Hydrogen Energy,* 2023.

[26] E. McKenna et M. Thomson, «High-resolution stochastic integrated thermal–electrical domestic demand model,» *Applied Energy,* vol. 165, pp. 445-461, 2016.

[27] I. Richardson, M. Thomson et D. Infield, «A high-resolution domestic building occupancy model for energy demand simulations,» *Energy and Buildings,* vol. 40, pp. 1560-1566, 2008.

[28] I. Richardson, M. Thomson, D. Infield et C. Clifford, «Domestic electricity use: A high-resolution energy demand model,» *Energy and Buildings,* vol. 42, p. 1878–1887, 2010.

[29] J. Barton, M. Thomson, P. Sandwell et A. Mellor, «A Domestic Demand Model for India,» p. 743 – 753, 2020.

[30] WAMAK, «Heat pump type AiWa 23 EVI H Out,» 2019.

[31] C. Ghenai, T. Salameh et A. Merabet, «Technico-economic analysis of off grid solar PV/Fuel cell energy system for residential community in desert region,» *International Journal of Hydrogen Energy,* vol. 45, p. 11460–11470, 2020.

[32] M. Yue, H. Lambert, E. Pahon, R. Roche, S. Jemei et D. Hissel, «Hydrogen energy systems: A critical review of technologies, applications, trends and challenges,» *Renewable and Sustainable Energy Reviews,* vol. 146, p. 111180, 2021.

[33] M. R. Ranjbar et S. Kouhi, «Sources' Response for supplying energy of a residential load in the form of on-grid hybrid systems,» *International Journal of Electrical Power & Energy Systems,* vol. 64, pp. 635-645, 2015.

[34] P. Corbo, F. Migliardini et O. Veneri, «Experimental analysis and management issues of a hydrogen fuel cell system for stationary and mobile application,» *Energy Conversion and Management,* vol. 48, pp. 2365-2374, 2007.

[35] J. Cardozo, N. Marx, L. Boulon et D. Hissel, «Comparison of Multi-Stack Fuel Cell System Architectures for Residential Power Generation Applications Including Electrical Vehicle Charging,» chez *2015 IEEE Vehicle Power and Propulsion Conference (VPPC)*, 2015.

[36] Y. Zhou, A. Ravey et M.-C. Péra, «Real-time cost-minimization power-allocating strategy via model predictive control for fuel cell hybrid electric vehicles,» *Energy Conversion and Management,* vol. 229, p. 113721, 2021.

[37] Clean Hydrogen Partnership, *Strategic Research and Innovation Agenda 2021-2027,* 2022.

[38] IRENA, *Green Hydrogen Cost Reduction: Scaling up Electrolysers to Meet the 1.5^{o}C Climate Goal ,*, Abu Dhabi, 2020.

[39] L. Gracia, P. Casero, C. Bourasseau et A. Chabert, «Use of Hydrogen in Off-Grid Locations, a Techno-Economic Assessment,» *Energies,* vol. 11, 2018.

[40] A. Kirubakaran, S. Jain et R. K. Nema, «A review on fuel cell technologies and power electronic interface,» *Renewable and Sustainable Energy Reviews,* vol. 13, pp. 2430-2440, 2009.

[41] J. Romdhane et H. Louahlia-Gualous, «Energy assessment of PEMFC based MCCHP with absorption chiller for small scale French residential application,» *International Journal of Hydrogen Energy,* vol. 43, pp. 19661-19680, 2018.

[42] O. Gudmundsson, J. Thorsen et L. Zhang, «Cost analysis of district heating compared to its competing technologies,» 2013.

[43] A. M. Ferrario, A. Bartolini, F. S. Manzano, F. J. Vivas, G. Comodi, S. J. McPhail et J. M. Andujar, «A model-based parametric and optimal sizing of a battery/hydrogen storage of a real hybrid microgrid supplying a residential load: Towards island operation,» *Advances in Applied Energy,* vol. 3, p. 100048, 2021.

[44] International Energy Agency (IEA), «The Future of Hydrogen, Seizing today's opportunities,» 2019.

[45] J. C. G. Parks et R. Remick, «Hydrogen Station Compression,Storage, and DispensingTechnical Status and Costs,» 2014.

[46] UK Department for Business, Energy & Industrial Strategy, *Energy Prices Domestic Prices, Average variable unit costs and fixed costs for electricity for regions in the United Kingdom,* 2021.

[47] V. M. Maestre, A. Ortiz et I. Ortiz, «Challenges and prospects of renewable hydrogen-based strategies for full decarbonization of stationary power applications,» *Renewable and Sustainable Energy Reviews,* vol. 152, p. 111628, 2021.

[48] Argonne National Laboratory, *GREET2,* 2022.

[49] Ministère de la Transition écologique, «La mobilité bas-carbone: Choix technologiques, enjeux matières et opportunités industrielles,» 2022.

[50] V. Knop, *Life Cycle Analysis of hydrogen storage tanks,* 2022.

[51] C. Robert, A. Ravey, R. Perey et D. Hissel, «Environmental impacts of batteries for transportation application according to different life cycle steps,» chez *2022 IEEE Vehicle Power and Propulsion Conference (VPPC)*, 2022.

[52] R. Frischknecht, R. Itten et F. Wyss, «Life Cycle Assessment of Future Photovoltaic Electricity Production from Residential-scale Systems Operated in Europe,» 2015.

[53] Electricity maps, *Electricity maps Database,* 2022.

[54] MATLAB, version 9.10.0.1710957 (R2021b), Natick, Massachusetts: The MathWorks Inc., 2021.